The Size Distribution of the Neptune Trojans and the Missing Intermediate Sized Planetesimals

Scott S. Sheppard

Department of Terrestrial Magnetism, Carnegie Institution of Washington, 5241 Broad Branch Rd. NW, Washington, DC 20015
sheppard@dtm.ciw.edu

and

Chadwick A. Trujillo

Gemini Observatory
670 North A'ohoku Place, Hilo, HI 96720

ABSTRACT

We present an ultra-deep survey for Neptune Trojans using the Subaru 8.2-m and Magellan 6.5-m telescopes. The survey reached a 50% detection efficiency in the R-band at $m_R = 25.7$ magnitudes and covered 49 square degrees of sky. $m_R = 25.7$ mags corresponds to Neptune Trojans that are about 16 km in radius (assuming an albedo of 0.05). A paucity of smaller Neptune Trojans (radii < 45 km) compared to larger ones was found. The brightest Neptune Trojans appear to follow a steep power-law slope ($q = 5 \pm 1$) similar to the brightest objects in the other known stable reservoirs such as the Kuiper Belt, Jupiter Trojans and main belt asteroids. We find a roll-over for the Neptune Trojans that occurs around a radii of $r = 45 \pm 10$ km ($m_R = 23.5 \pm 0.3$), which is also very similar to the other stable reservoirs. All the observed stable regions in the the solar system show evidence for Missing Intermediate Sized Planetesimals (MISPs). This indicates a primordial and not collisional origin, which suggests planetesimal formation proceeded directly from small to large objects. The scarcity of intermediate and smaller sized Neptune Trojans may limit them as being a strong source for the short period comets.

Subject headings: Kuiper Belt – comets: general – minor planets, asteroi ds – solar system: general – planetary formation

1. Introduction

Our understanding of how objects in the early solar system coagulated to form planetesimals of the kilometer size scale is mostly limited to theory (Bottke et al. 2005; Johansen et al. 2007; Blum & Wurm 2008; Cuzzi et al. 2008; Morbidelli et al. 2009). Though we can detect some gas and dust disks as well as large planets around stars, we will not be able to detect extra-solar planetesimals on the kilometer to thousands of kilometer size scale in the foreseeable future. Currently, the only way to directly study such a population is through the stable reservoirs in our solar system (Jewitt et al. 2000; Kenyon & Bromley 2004; Pan & Sari 2005; Bottke et al. 2005; Fraser & Kavelaars 2008; Fuentes & Holman 2008; Fraser et al. 2008; Fuentes et al. 2009; Fraser 2009; Morbidelli et al. 2009). The orbits of objects in the main asteroid belt, Kuiper belt and Trojan regions have been highly influenced by the migration and evolution of the Solar System. Since Trojan asteroids share their planet's orbital period and semi-major axis they are especially useful in constraining the formation and migration of their planet (Morbidelli et al. 2005; Tsiganis et al. 2005). Trojan asteroids lead (L4) or trail (L5) a planet by about sixty degrees near the two triangular Lagrangian points of gravitational stability. The Jupiter Trojans have been known since Max Wolf discovered 588 Achilles in 1906. There are currently about 3000 known Trojans in the L4 and L5 regions of Jupiter. Neptune's first Trojan was discovered within the L4 region in 2001 while several more Neptune Trojans have been discovered in recent years (Chiang et al. 2003; Sheppard & Trujillo 2006, 2010; Becker et al. 2008). The other giant planets Saturn and Uranus are not expected to have a significant number of Trojans since their Lagrangian regions are more dynamically unstable over the age of the solar system (Nesvorny & Dones 2002).

The dynamics of Kuiper Belt objects in outer mean-motion resonances with Neptune, such as the 3:2 and 2:1 resonances, suggest that Neptune likely migrated several AU outwards during its lifetime (Hahn & Malhotra 2005; Chiang & Lithwick 2005; Levison et al. 2008). Similarly, the Hildas in the main asteroid belt are in the 2:3 mean-motion resonance with Jupiter and their orbital distribution suggests Jupiter migrated inward by a few tenths of AU (Franklin et al. 2004). Unlike these inner and outer resonance objects, the Trojans, which are in a 1:1 resonance with their respective planet, would likely have been depleted during any large, irregular planetary migration. The capture of Trojans in the current Solar System is not an effective process and thus capture happened when the Solar System dynamics were significantly different than now (Horner & Evans 2006). Thus the Trojans were likely captured during either a slow smooth planetary migration process or more likely after any significant planetary migration through a Neptune freeze-in circularization process (Kortenkamp et al. 2004; Morbidelli et al. 2005; Sheppard & Trujillo 2006; Li et al. 2007; Nesvorny & Vokrouhlicky 2009; Lykawka et al. 2009). Both the L4 and L5 Neptune Trojan regions appear to have similar sized populations and dynamics. The expected large number

of high inclination Neptune Trojans in both the L4 and L5 regions of Neptune suggests that capture occurred with a dynamically excited planetesimal population (Sheppard & Trujillo 2010).

2. Observations

Observations were obtained in June 2008 and 2009 for the L5 region and October 2004-2009 for the L4 region of Neptune. For the Subaru observations the Suprime-Cam with ten 2048×4096 pixel CCDs arranged in a 5×2 pattern was used. Suprime-Cam has 15μm pixels that gives a pixel scale of $0.''20$ pixel^{-1} at prime focus and a field-of-view that is about $34' \times 27'$ with the North-South direction aligned with the long axis. Gaps between the chips are about $16''$ in the North-South direction and $3''$ in the East-West direction (Miyazaki et al. 2002). At Magellan the the IMACS camera on the Baade telescope was used. IMACS is a wide-field CCD imager that has eight 2048×4096 pixel CCDs with a pixel scale of $0.''20$ pixel^{-1} and a field-of-view of about 0.2 square degrees. The eight CCDs are arranged in a 4×2 box pattern with four above and four below and about 12 arcsecond gaps between chips.

The images were bias-subtracted and then flat-fielded with twilight flats. During exposures the telescope was autoguided sidereally on field stars. Integration times were between 300 and 450 seconds and images of the same field were obtained on three visits with 1 to 1.5 hours between visits. Observations were obtained while the Neptune Trojans were within 1 hour of opposition so the dominant apparent motion was largely parallactic and thus is inversely related to distance. Objects at the heliocentric distance of Neptune, $R \sim 30$ AU, will have an apparent motion of about $\sim 4''$ hr^{-1}.

3. Results and Analysis

Previous surveys for Neptune Trojans focused mostly on finding relatively bright objects (radii greater than 40 km or brighter than 24th magnitude) (Chiang et al. 2003; Sheppard & Trujillo 2006; Becker et al. 2008). The Neptune Trojan regions cover thousands of square degrees on the sky as many Trojans have large inclinations and librate up to ± 30 degrees from the Lagrangian points over a ten thousand year time scale (Chiang et al. 2003). We obtained an ultra-deep, large area survey of the Neptune L5 and L4 Trojan regions. A total of 49 square degrees were searched of which 30 square degrees were in the L4 region while the other 19 square degrees were in the L5 region of Neptune. Subaru was used to covered 21

square degrees while Magellan was used for the other 28 square degrees of the survey. The first high inclination Neptune Trojan, 2005 TN_{53}, was discovered at Magellan (Sheppard & Trujillo 2006) while the first L5 Neptune Trojan (2008 LC_{18}: Sheppard & Trujillo 2010) was found at Subaru. In all, five L4 Neptune Trojans were detected at Magellan ranging from 22.5 to 23.7 magnitudes (about 70 to 40 km in radius) while one L5 Neptune Trojan was detected at Subaru with an magnitude of 23.2 in the R-band.

The data were analyzed with a computer algorithm tuned to detect objects which appeared in all three images from one night with an apparent motion consistent with being beyond the orbit of Jupiter (speeds less than 20 arcseconds per hour). Objects were flagged as possible Neptune Trojans if they moved between 3.5 and 4.5 arcseconds per hour. These objects were recovered up to two months later to determine if they had Neptune Trojan like orbits. The survey was designed similar to our ultra-deep surveys for satellites around the planets (Sheppard et al. 2005; Sheppard & Trujillo 2009).

We determined the limiting magnitude of the survey by placing artificial objects in the fields matched to the point spread function of the images and with motions of 4 arcseconds per hour. The brightnesses of the objects were binned by 0.1 mag and spanned the range from 25 to 27 magnitudes. Results are shown in Figure 1. The 50% detection efficiency for most of the fields is taken as our limiting magnitude, found to be $m_R = 25.7$. Radii (r) of the Neptune Trojans were determined assuming an albedo of $\rho_R = 0.05$ and using the equation, $r = (2.25 \times 10^{16} R^2 \Delta^2 / p_R \phi(0))^{1/2} 10^{0.2(m_\odot - m_R)}$ where R is the heliocentric distance in AU, Δ is the geocentric distance in AU, $m_\odot$ is the apparent red magnitude of the sun (-27.1), p_R is the red geometric albedo, m_R is the apparent red magnitude of the Trojan and $\phi(0) = 1$ is the phase function at opposition. Using an albedo of 0.05 (Fernandez et al. 2003; Fernandez et al. 2009) we find that 25.7 magnitudes corresponds to a Neptune Trojan with a radius of about 16 km.

The Cumulative Luminosity Function (CLF) describes the sky-plane number density of objects brighter than a given magnitude. The CLF can be described by

$$\log[\Sigma(m_R)] = \alpha(m_R - m_o) \quad (1)$$

where $\Sigma(m_R)$ is the number of objects brighter than m_R, m_o is the magnitude zero point, and α describes the slope of the luminosity function. The CLF found for Neptune Trojans is shown in Figure 2. The CLF of the brightest Neptune Trojans ($m_R < 23.5$ magnitude) follows a steep power law of $\alpha \sim 0.8$ similar to the brightest Kuiper Belt objects, Jupiter Trojans and main belt asteroids (Jewitt et al. 2000; Jedicke et al. 2002; Bottke et al. 2005; Fraser & Kavelaars 2008; Fuentes & Holman 2008). The Neptune Trojans discovered in our survey are all bright ($m_R < 23.7$ magnitudes) compared to the limiting magnitude of many of the survey fields ($m_R = 25.7$ magnitudes). A roll-over in the Neptune Trojan CLF is

apparent around $m_R = 23.5 \pm 0.3$. For the Neptune Trojans the best fit to the CLF for $m_R < 23.5$ mag is $\alpha = 0.8 \pm 0.2$ and $m_o = 24.45 \pm 0.4$.

The points in a CLF are heavily correlated with one another, tending to give excess weight to the faint end of the distribution. The Differential Luminosity Function (DLF) does not suffer from this problem. We plot the DLF using a bin size of 0.5 mag for all Neptune Trojans detected in our survey (Figure 3). The roll-over in the number of fainter objects is shown more dramatically through the DLF, and is insensitive to bin size choice. If the fainter (smaller) objects continued to follow the $q = 5$ size distribution slope of the brighter (larger) objects we would have expected to discover 80±10 Neptune Trojans between the roll-over point at $m_R \sim 23.5$ magnitudes ($r \sim 45$ km) and our survey limit of $m_R \sim 25.7$ magnitudes ($r \sim 16$ km). Though we found hundreds of Kuiper Belt objects with $m_R > 24$ magnitudes we found zero Neptune Trojans of this faintness, which gives about an 8σ result that the smaller Neptune Trojans have a shallower power-law slope than the larger Neptune Trojans.

Thus like the other known stable small body reservoirs, the CLF of the Neptune Trojans is best fit by a broken power law that breaks from a steep slope for the largest objects to a shallow distribution for the smaller objects. The data at the faintest end for the Neptune Trojans are within about 2σ of the shallow slope found for faint KBOs (Figure 2). Further data are required to determine a reliable slope for the Neptune Trojans at the faint end of the CLF. Though we cannot completely rule out the possibility that the Neptune Trojans have a single very shallow power law it seems unlikely since we cannot fit a single power law to all the points to within 1σ and the best fit power law to all the data would be the shallowest observed ($q \sim 2.5$) for such relatively large objects in the solar system. This slope would also be much shallower than the Dohnanyi slope of 3.5 that is expected if the objects were in a state of collisional equilibrium (O'Brien & Greenberg 2003).

4. Size Distribution

One of the main ways to constrain the formation and collisional history of an ensemble of objects such as the Neptune Trojans is to determine their size distribution. The size distribution is an indicator of how the accretion process worked and is related to the CLF. If we assume the Neptune Trojans all have similar albedos to the Jupiter Trojans (0.05, Fernandez et al. 2003) and are at a distance of 30 AU we can determine the size distribution (Figure 4) of the Neptune Trojans from the CLF. A slope of $q = 5 \pm 1$ is found for the large Neptune Trojan size distribution, where $n(r)dr \propto r^{-q}dr$ is the differential power-law radius distribution with $n(r)dr$ the number of Neptune Trojans with radii in the range r to $r + dr$.

The roll-over in the size distribution for the Neptune Trojans occurs around a radius of 45 ± 10 km. When compared to the Kuiper Belt (Bernstein et al. 2004; Fraser & Kavelaars 2008; Fuentes & Holman 2008; Schlichting et al. 2009) and Jupiter Trojan (Jewitt et al. 2000; Yoshida & Nakamura 2005; Yoshida & Nakamura 2008) size distributions it appears that all three outer solar system small body populations have a similar roll-over in their size distribution (radii of 35 ± 5, 40 ± 15 km respectively for the Jupiter Trojans and Kuiper Belt). Previous authors have shown that the Kuiper Belt's low inclination and high inclination classical populations may have different initial size distributions (Bernstein et al. 2004; Fuentes & Kavelaars 2008; Morbidelli et al. 2009). The Neptune Trojans have a steep size distribution at the large end, similar to that found for the low inclination Kuiper Belt objects and Jupiter Trojans, which may hint at a common origin (Morbidelli et al. 2009). Further, the main belt of asteroids (Jedicke et al. 2002; Bottke et al. 2005) has a similar roll-over as the above reservoirs around a radius of 50 ± 5 km.

4.1. Missing Intermediate Sized Planetesimals (MISPs)

There are unexpectedly far fewer tens of kilometer sized objects than larger objects in all the known stable reservoirs of small bodies in our solar system. The Missing Intermediate Sized Planetesimals (MISPs) are either an indication that the intermediate sized objects have been collisionally eroded over the age of the solar system or a primordial distribution deficient in intermediate sized objects was in place before capture. MISPs are not expected from a uniformly accreted population (Bottke et al. 2005; Kenyon et al. 2008). Detailed numerical collisional simulations (Morbidelli et al. 2009) have shown that collisional grinding is not the likely cause of the roll-over around a radius of 50 km in the size distribution of the main belt asteroids. This suggests the roll-over is a consequence of the original primordial formation mechanism of planetesimals. Further, considering that each of the different small body reservoirs have significantly different compositions and collisional histories, the similarities of all the MISPs sizes throughout the various reservoirs suggests the lack of intermediate sized objects is likely a primordial result from before the planets formed. This has far-reaching implications for planetesimal formation and is very important for understanding planet formation in general. It is currently not understood how objects larger than about a meter in size formed in the solar nebula since meter-sized objects are likely to be disrupted from collisional erosion and have very short dynamical lifetimes due to gas drag and thus should not be able to grow to larger sizes (Wurm et al. 2005; Cuzzi & Weidenschilling 2006; Dominik et al. 2007; Blum et al. 2008). Several recent papers have suggested that the planetesimal formation mechanism jumps over this meter size barrier and instead large objects of hundreds of kilometers in size coalesce directly from over-dense clouds of cm to

meter sized particles in a highly turbulent primordial solar nebula (Johansen et al. 2007; Cuzzi et al. 2008; Morbidelli et al. 2009; Johansen et al. 2009).

Numerical collisional simulations as performed for the main asteroid belt (Morbidelli et al. 2009) and their effect on the size distribution for the outer solar system small body reservoirs are warranted to constrain the role collisions play in helping produce the observed size distributions in these locations. It is likely that the Trojans and Kuiper Belt objects have undergone less collisional evolution than the main belt asteroids since emplaced in their current orbits (Kenyon et al. 2008; Morbidelli et al. 2009; Levison et al. 2009) and if confirmed would indicate the observed roll-over in their size distribution is likely from primordial formation of the planetesimals. In addition, the outer Solar System objects are likely to have some material strength (Levison et al. 2009; Leinhardt & Stewart 2009), which appears to be an impediment for collisional erosion to account for the observed roll-over in the Kuiper Belt size distribution (Pan and Sari 2005). To date the size distributions of these more distant outer solar system reservoirs are much more poorly characterized by observations as the main asteroid belt.

Detailed in this work is the first measurement of the size distribution for the Neptune Trojans. The observations in this work, when compared with limited collisional simulations (Morbidelli et al. 2009), show that the lack of objects tens of kilometers in size for all known reservoirs agrees with planetesimal formation skipping over forming significant numbers of objects in the tens of kilometer size range for all areas of the Solar System. In this scenario, objects smaller than about $r \sim 35 - 50$ km are most likely collisional by-products of larger primordial objects (Farinella & Davis 1996; Kenyon & Bromley 2004; Kenyon et al. 2008). It is possible that future collisional simulations using size-dependent drift due to the drag of a low turbulent solar nebular gas during accretion could account for the observed roll-over (Weidenschilling 2010) in the size distributions, but this scenario would likely be much more dependent on formation location in the solar nebula unlike the primordial coalescence of large objects from over-dense dust clouds.

4.2. Small Body Reservoir Populations

Comparing the various observed small body reservoirs shows that the Kuiper Belt holds most of the objects larger than 50 km in radius, about $150,000$. The Neptune Trojans are the next most populated reservoir with about 400 objects larger than 50 km in radius expected (a factor of about 375 less than the Kuiper Belt). The main belt asteroids contain about 200 objects larger than 50 km in radius or a factor of 2 less than the Neptune Trojans. The Jupiter Trojans have about 50 objects this size or a factor of 8 less than the Neptune

Trojans.

Acknowledgments

We thank J. Chambers for comments on this manuscript. Based in part on data collected at Subaru Telescope, which is operated by the National Astronomical Observatory of Japan. This paper includes data gathered with the 6.5 meter Magellan Telescopes located at Las Campanas Observatory, Chile. C.T. was supported by the Gemini Observatory, which is operated by the Association of Universities for Research in Astronomy, Inc., on behalf of the international Gemini partnership of Argentina, Australia, Brazil, Canada, Chile, the United Kingdom, and the United States of America. S. S. was supported in part by funds from the NASA New Horizons Spacecraft Pluto mission.

REFERENCES

Becker, A. et al. 2008, ApJ, 682, L53

Bernstein, G. et al. 2004, AJ, 128, 1364

Blum, J. & Wurm, G. 2008, Ann. Rev. of Astr. & Astrophys., 46, 21

Bottke, W., Durda, D., Nesvorny, D., et al. 2005, Icarus, 175, 111

Chiang, E. & Lithwick, Y. 2005, ApJ, 628, 520

Chiang, E. et al. 2003, AJ, 126, 430

Cuzzi, J., & Weidenschilling, S. 2006, in Meteorites and the Early Solar System II, eds. D. Lauretta & H. McSween, (Tucson, Az: Univ. Arizona Press) 353-381

Cuzzi, J., Hogan, R., & Shariff, K. 2008, AstroPhys. J., 687, 1432

Dominik, C., Blum, J., Cuzzi, J., & Wurm, G. 2007, in Protostars and Planets V, eds. B. Reipurth et al. (Tucson, Az: Univ. Arizona Press) 783-800

Farinella, P. & Davis, D. 1996, Science, 273, 938-941

Fernandez, Y., Jewitt, D., & Ziffer, J. 2009, AJ, 138, 240

Fernandez, Y., Sheppard, S., & Jewitt, D. 2003, AJ, 126, 1563

Franklin, F., Lewis, N., Soper, P., & Holman, M. 2004, AJ, 128, 1391

Fraser, W. & Kavelaars, J. 2008, Icarus, 198, 452

Fraser, W. et al. 2008, Icarus, 195, 827

Fraser, W. 2009, ApJ, 706, 119

Fuentes, C. & Holman, M. 2008, AJ, 136, 83

Fuentes, C., George, M., & Holman, M. 2009, ApJ, 696, 91

Hahn, J. & Malhotra, R. 2005, AJ, 130, 2392

Horner, J. & Evans, W. 2006, MNRAS, 367, L20

Jedicke, R., Larsen, J. & Spahr, T. 2002, in Asteroids III, eds. W. Bottke et al. (Tucson, Az: Univ. Arizona Press) 71-88

Jewitt, D., Trujillo, C., & Luu, J. 2000, AJ, 120, 1140

Johansen, A. et al. 2007, Nature, 448, 1022

Johansen, A., Youdin, A. & Mac Low, M. 2009, 704, L75

Kenyon, S. & Bromley, B. 2004, AJ, 128, 1916

Kenyon, S. et al. 2008, in The Solar System Beyond Neptune, eds. M. A. Barucci et al. (Tucson, Az: Univ. Arizona Press) 293-313

Kortenkamp, S., Malhotra, R., & Michtchenko, T. 2004, Icarus, 167, 347

Leinhardt, Z. & Stewart, S. 2009, Icarus, 199, 542

Levison, H. et al. 2009, Nature, 460, 364

Levison, H., Morbidelli, A., Vanlaerhoven, C., Gomes, R., & Tsiganis, K. 2008, Icarus, 196, 258

Li, J., Zhou, L., & Sun, Y. 2007, AA, 464, 775

Lykawka, P., Horner, J., Jones, B., & Mukai, T. 2009, MNRAS, 398, 1715

Miyazaki, S. et al. 2002, PASJ, 54, 833

Morbidelli, A., Bottke, W., Nesvorny, D., & Levison, H. 2009, Icarus, 204, 558

Morbidelli, A., Levison, H., Tsiganis, K., & Gomes, R. 2005, Nature, 435, 462

Morbidelli, A. et al. 2009, Icarus, 202, 310

Nesvorny, D. & Dones, L. 2002, Icarus, 160, 271

Nesvorny, D. & Vokrouhlicky, D. 2009, AJ, 137, 5003

O'Brien, D. & Greenberg, R. 2003, Icarus, 164, 334

Pan, M. & Sari, R. 2005, Icarus, 173, 342

Schlichting, H. et al. 2009, Nature, 462, 895

Sheppard, S., Jewitt, D.,& Kleyna, J. 2005, AJ, 129, 518

Sheppard, S. & Trujillo, C. 2006, Science, 313, 511

Sheppard, S. & Trujillo, C. 2009, Icarus, 202, 12

Sheppard, S. & Trujillo, C. 2010, Science, 329, 1304

Tsiganis, K., Gomes, R., Morbidelli, A., & Levison, H. 2005, Nature, 435, 459

Weidenschilling, S. 2010, Lunar Planet. Inst. Sci. Conf., 41, 1453

Wurm, G., Paraskov, G., & Krauss, O. 2005, Icarus, 178, 253

Yoshida, F. & Nakamura, T. 2005, AJ, 130, 2900

Yoshida, F. & Nakamura, T. 2008, PASJ, 60, 297

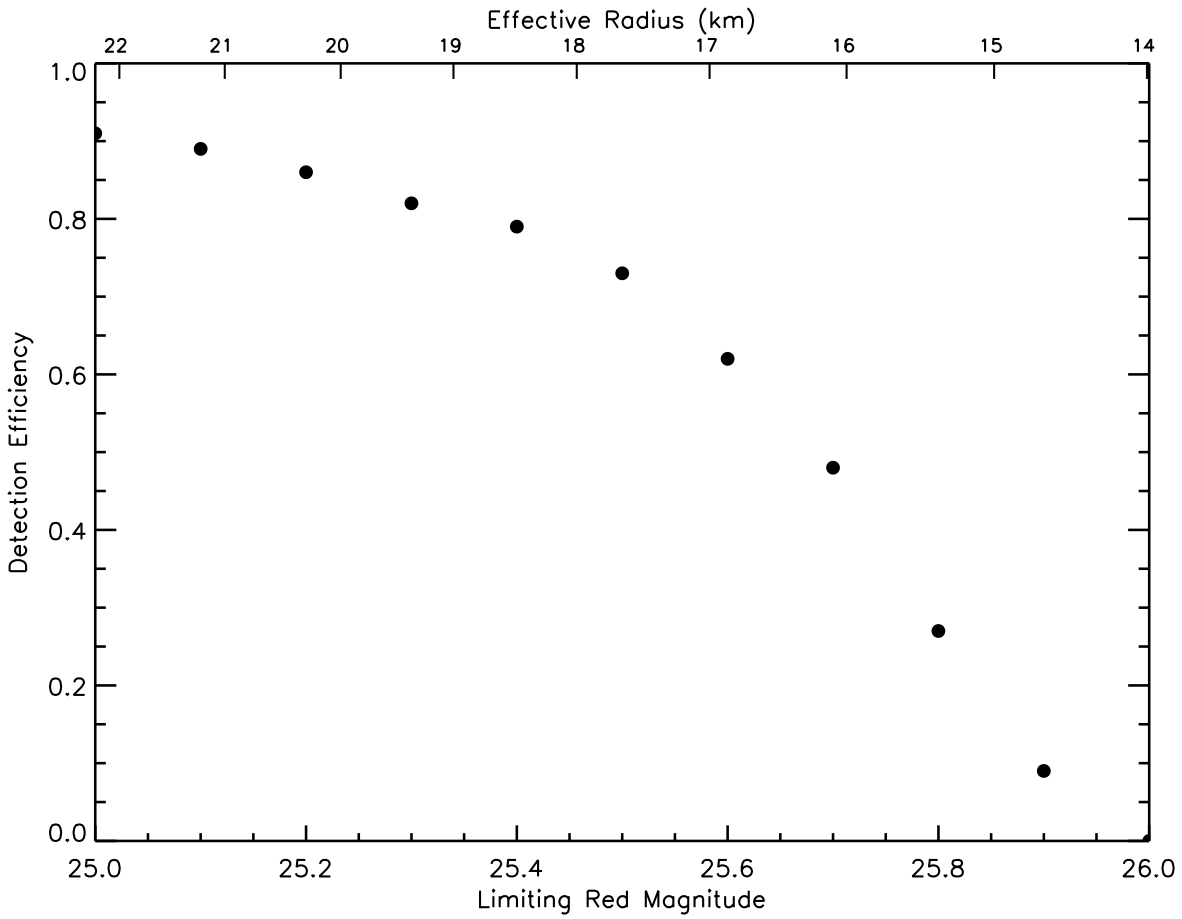

Fig. 1.— Detection efficiency of the Neptune Trojan survey versus apparent red magnitude. The 50% detection efficiency is at an R-band of 25.7 magnitudes as determined by our computer algorithm's performance on implanted artificial moving objects at Neptune Trojan apparent velocities. Effective radii of the apparent magnitude were calculated assuming an albedo of 0.05.

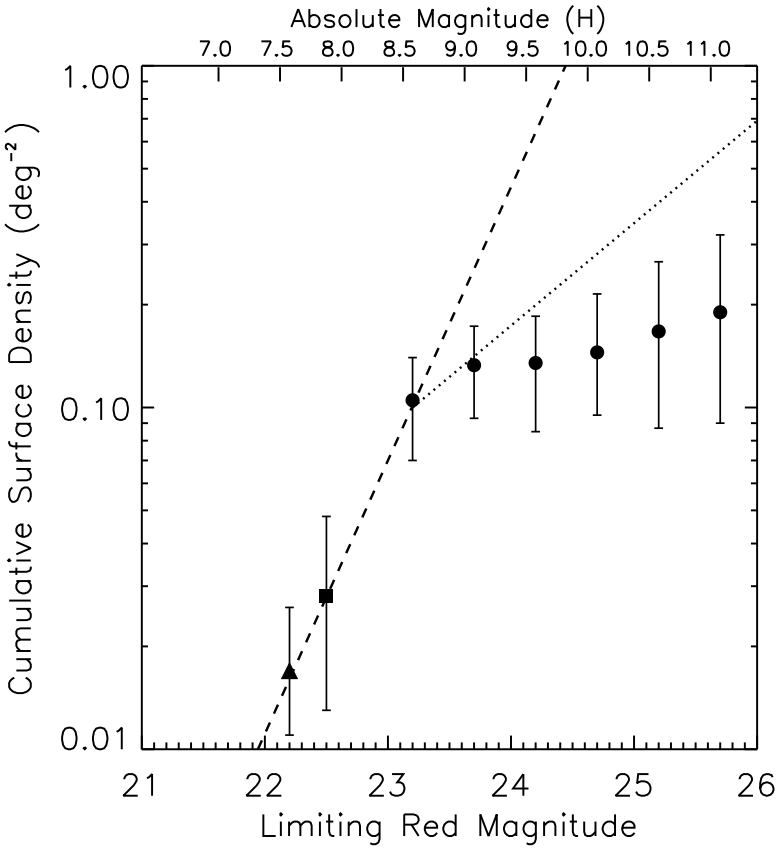

Fig. 2.— The Cumulative Luminosity Function (CLF) of the Neptune Trojans, where the black circles are this work, the square is from the Deep Ecliptic Survey (DES: Chiang et al. 2003) and the triangle is from the Sloan Digital Sky Survey (SDSS: Becker et al. 2008). A steep power law slope ($\alpha = 0.8 \pm 0.2$ ($q = 5 \pm 1$)), which is similar to what has been found for the largest objects in the main asteroid belt, Jupiter Trojans and Kuiper Belt, is plotted as a dashed line and fits the bright end of the Neptune Trojans CLF. A roll-over in the Neptune Trojan CLF is apparent around $m_R = 23.5 \pm 0.3$. The dotted line shows a shallow power law slope of $\alpha = 0.3$ ($q = 2.5$) found for the intermediate to smaller sized KBOs (Fraser & Kavelaars 2008; Fuentes & Holman 2008). The data at the faintest end for the Neptune Trojans are within about 2σ to the shallow slope found for faint KBOs. No Neptune Trojans were discovered fainter than 23.7 magnitudes. The black circles do not follow a flat horizontal line when fainter than about 24th magnitude since a smaller area was covered at fainter magnitudes due to variable seeing conditions on a few nights.

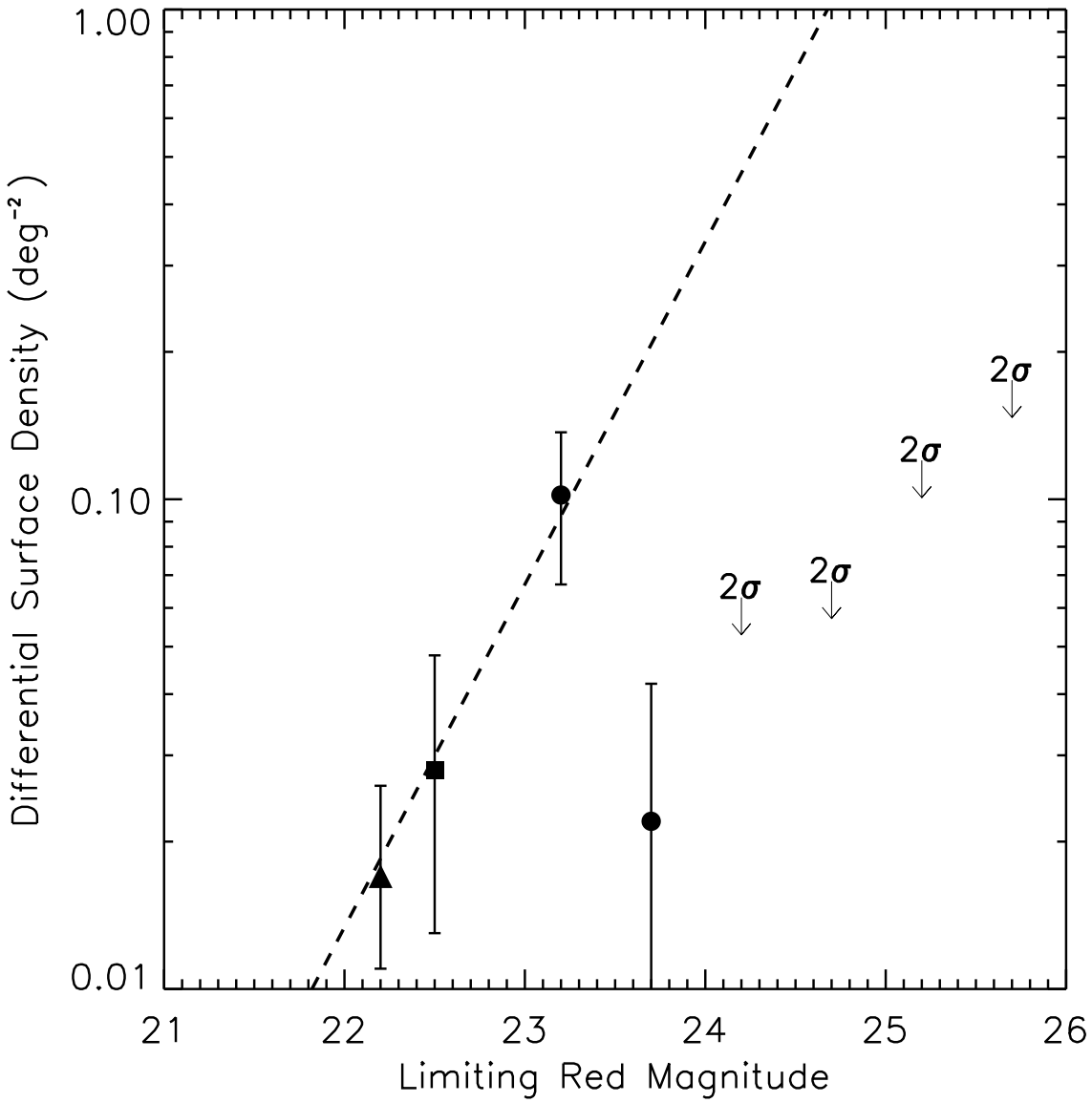

Fig. 3.— The Differential Luminosity Function (DLF) of the Neptune Trojans where the black circles are this work, the square is from the Deep Ecliptic Survey (DES: Chiang et al. 2003) and the triangle is from the Sloan Digital Sky Survey (SDSS: Becker et al. 2008). The 2σ upper limits are shown for non-detections at fainter magnitudes where no objects were found in this work. It is apparent that there are fewer fainter objects than brighter objects.

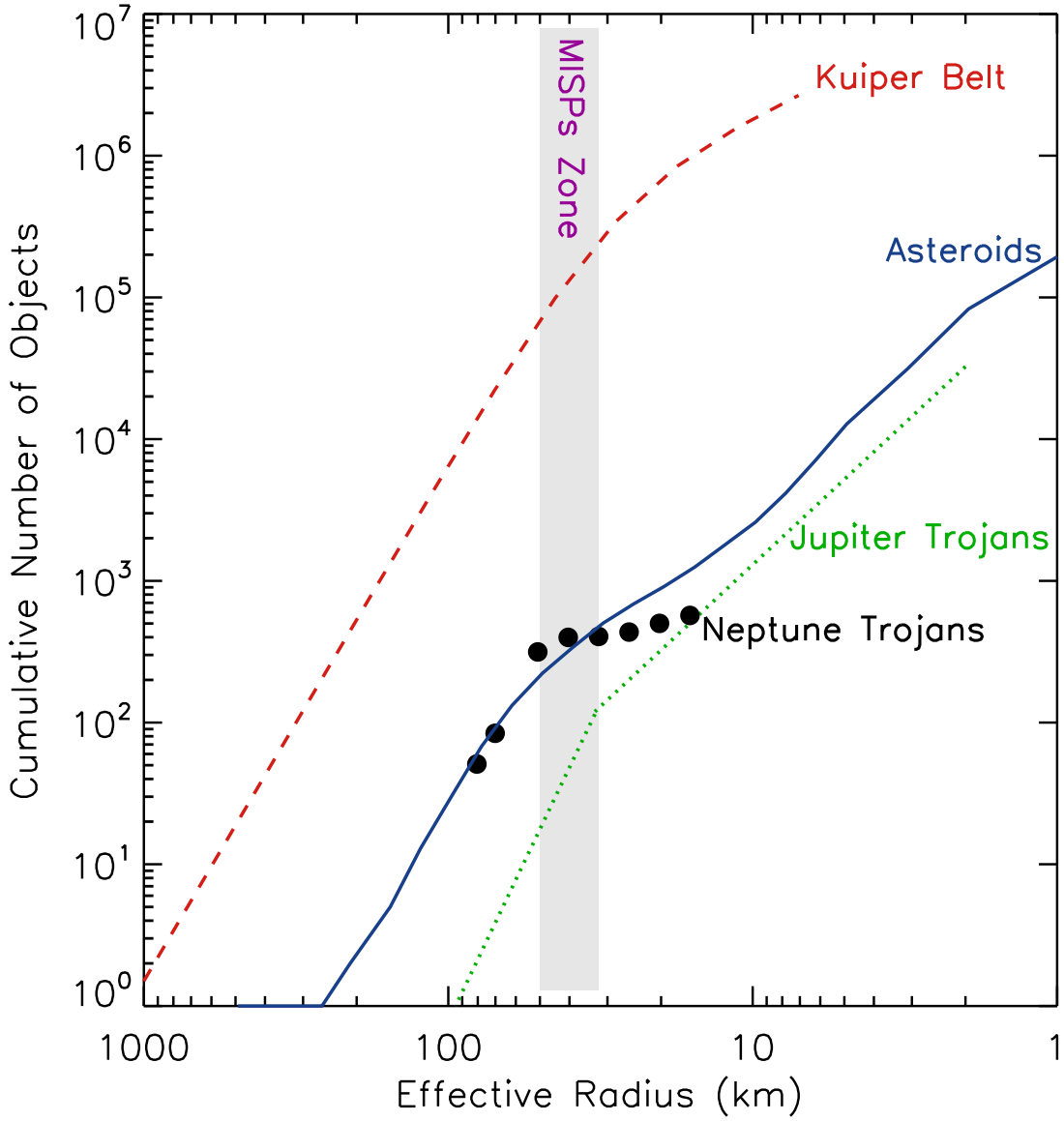

Fig. 4.— The cumulative size distribution of the Neptune Trojans (black circles; from the SDSS, DES and this work which includes both the L4 and L5 clouds), Jupiter Trojans (Jewitt et al. 2000) (green dotted line; including both the L4 and L5 clouds), Kuiper Belt objects (Fraser and Kavelaars 2008; Fuentes and Holman 2008) (red dashed line) and main belt asteroids (Jedicke et al. 2002; Bottke et al. 2005) (blue solid line). All four small body reservoirs have a similar steep slope for the largest objects size distribution ($q \sim 5$). Though the objects in each reservoir likely have significantly different compositions, internal structures and collisional histories they all have a roll-over in their size distributions between about 35 and 50 km in radius, which we call the Missing Intermediate Sized Planetesimals (MISPs). The similar size of the roll-over for each stable reservoir favors a primordial instead of a collisional formation. The error bars for the Neptune Trojan points have been removed for clarity but would be similar as in Figure 2.